THIONE-THIOL TAUTOMERIC EQUILIBRIUM IN A DIHYDROPYRIMIDINE-THIONE: X RAY DIFFRACTION HELPED BY NMR, FTIR AND THEORETICAL CALCULATIONS

L. ÁLVAREZ [1], F. BROVELLI [2], R. BAGGIO [3], O. PEÑA [4], J. MUÑOZ [5], J. SOTO-DELGADO [5] AND Y. MORENO [6]*

[1]*Universidad Técnica Federico Santa María, Valparaiso, Chile.*
[2]*Universidad de Concepción, Escuela de Educación, Depto Cs. Básicas, Los Angeles, Chile.*
[3]*GIyA, Centro Atómico Constituyentes, Comisión Nacional de Energía Atómica, Buenos Aires, Argentina.*
[4]*Institut des Sciences Chimiques de Rennes, UMR 6226, Université de Rennes-1, Rennes, France.*
[5]*Universidad Andrés Bello, Departamento de Química, Facultad de Ciencias Exactas, Viña del Mar, Chile.*
[6]*Facultad de Ciencias, Departamento de Química, Universidad de La Serena, La Serena, Chile.*

ABSTRACT

The solid state *thione-thiol* equilibrium in 4,6-di-phenyl-3,4-di-hydro-pyrimidine-2(1H)-thione ($C_{16}H_{14}N_2S$) is analyzed through three different techniques, viz: Single Cristal X-Ray Diffraction (SCXRD), Nuclear Magnetic Resonance (NMR) and Fourier Transformed Infra-Red spectroscopy (FTIR), each one providing complementary information to the solution of the problem. The existence of *thione-thiol* equilibrium is firmly established, both in solution (by HNMR techniques) as in the solid state (by FTIR methods), and even if no traces of the *thiol* form could be found via SCXRD, some hints about the way in which the coexistence of both forms could be structurally achieved are provided by the structural analysis. In order to confirm the existence of this equilibrium, theoretical calculations were carried out at the B3LYP/6-311G(d,p) level theory, and a double proton transfer reaction is proposed.

Keywords: Greywater, Microfiltration, ultrafiltration, bio reactors, filtering membranes.

1. INTRODUCTION

Heterocyclic compounds, such as pyrimidine derivatives are present in different natural products (Zeng *et al*., 2003, Zhang *et al*., 2014; Kachroo *et al.*, 2014), exhibiting a variety of chemical and physical properties which convert them into an attractive source of research materials for synthetic heterocyclic chemistry, analytical chemistry and pharmacology (Trivedi *et al*., 2015; Gupta & Gupta, 2015).

The structural knowledge of these compounds relays heavily in single crystal X-ray diffraction, whose extreme efficiency is beyond any doubt as confirmed by the rapidly expanding contents of the CSD (Version 5.38 and upgrades, Groom *et al.*, 2016).

There are, however, some challenges in the structural study of these natural product for which the technique of single crystal X-ray diffraction (SCXRD) finds rather difficult, or even impossible, to tackle on its own, viz., the determination of the correct chirality in the absence of medium weight atoms, or the "trapping" of a flipping H in a case of tautomeric equilibrium (Stoyanov *et al.*,1990). Both queries are difficult to answer if only X-ray diffraction is used.

We have come across a problem which simultaneously shows the strengths and the weaknesses of the method, exemplified in the accurate structural study of an imidazole derivative of our interest: 4,6-di-phenyl-3,4-di-hydro-pyrimidine-2(1H)-thione (I).

The synthesis of this compound involves a two-stage process: the first one is the obtainment of a chalcone through an Aldol condensation, followed by a second step where the chalcone undergoes a nucleophilic attack by thio-urea. There are two possible outcomes out of this thio-urea attack, both of which consist in a condensation ring with either a S or a N atom embedded in the heterocycle. In our case, only one synthetic product was detected by TLC chromatography, and X-ray diffraction easily solved on its own this S *vs*. N controversy by assigning, beyond any doubt the N character to the hethero atom. Even if this result had previously been determined by NMR techniques, the SCXRD resolution did not relay on these results, and this (albeit modest) achievement should be considered as an X-ray successful outcome.

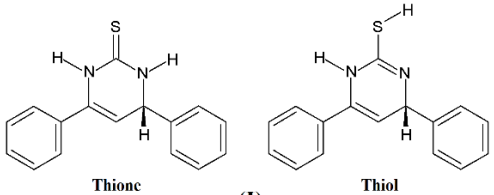

(I)

Scheme 1

But in addition to this issue, the synthesis of these compounds may present an additional challenge; viz., they can give rise to tautomeric equilibria (see Scheme 1). Even if the phenomenon is easy to detect in solution (in fact, ^{1}H NMR analysis had already determined the presence of both forms in a $CDCl_3$ solution of I) it is not so evident to trace it in the solid state. In the present case, and in spite of our extremely careful determination of the crystal and molecular structure of I (*), no observable traces of any kind of H delocalization could be found by SCXRD. However, as explained below, FTIR measurements showed otherwise, with what the existence of a *thione-thiol* tautomeric equilibrium was definitely established.

In this scenario, the following multidisciplinary study of 4,6-di-phenyl-3,4-di-hydro-pyrimidine-2(1H)-thione (I) could be considered a case of cooperative synergy, where various complementary techniques (unable on their own to find the complete solution) cooperate in a constructive way to find the best of possible answers.

(*) NOTA BENE: our R factor at 170 K was 0.027. A resolution of the same structure (at R.T. and with a slightly larger R index of 0.0464) has been mentioned in Kong *et al*., 2004 (CSD code: DALFUS). However, no further analysis or structural details are provided in the report, short of the CIF deposition.

2. EXPERIMENTAL

2.1. Instrumental techniques

1H NMR spectra (in CDCl3 solution) were recorded on an AVANCE 400 Digital Bruker NMR spectrometer (chemical shifts referenced to residual solvent peaks, δTMS= 0).

FTIR analysis was performed with an IR Prestige-21 Fourier Transform Infrared Spectrophotometer Shimadzu.

Single crystal X-ray diffraction data were collected on a Bruker SMART AXS CCD diffractometer using Mo Ka radiation (λ = 0.71073 Å).

2.2. Synthesis and crystallization

As ditto, the two-steps synthetic route to (I) consists of a chalcone generation and its later attack with thio-urea, with an (in principle uncertain) outcome: S or N in the cyclation product. The synthesis described below led to the N containing heterocycle.

4,6-di-phenyl-3,4-di-hydro-pyrimidine-2(1H)-thione

50 mL of 10% KOH solution was refluxed and 6.78 g (63.8 mmol) of benzaldehide was added; then 4.12 g (34.3 mmol) of acetofenone and 3.93 g (51.7 mmol) of thio-urea were added. After two hours of reaction the solvent is removed under vacuo; the product is filtered and washed with copious hot water

*Corresponding author email: yanko.moreno@userena.cl

and then with cold ethanol, yielding 2.87 g of a white solid (33% yield). 1H NMR (CDCl3)(multiplicity, integration, assignment according to Fig 1): δ 1.6956 (s, 1H, HS), 5,2026 (dt, J = 3.8, 2.0 Hz, 1H, HC4), 5.2890 (dd, J = 3.7, 1.6 Hz, 1H, HC3), 6.9844 (s, 1H, HN3), 7.3265-7.4414 (m, 10H, H—C Ar), 7.7209 (s, 1H, HN1).

2.3. Refinement

All H atoms attached to C were identified in an intermediate difference map, further idealized and allowed to ride both in coordinates as in displacement factors, the latter taken as U(H)= x U~equiv~(C), with C—H =0.93Å, x=1.2. Trying to help in sorting out the *thiol-thione* controversy, an extremely careful analysis around nitrogen and sulfur atoms was performed, but only N—H groups could be confidently individualized, whose H components were refined freely.

2.4. Computational details

DFT computations were carried out using the B3LYP/6-311G(d,p) level of theory. The Cartesian coordinates obtained from the X-ray structure determination were used as the starting geometry for the theoretical calculations. The stationary points were characterized by frequency computations in order to verify that transition states (TSs) have one and only one imaginary frequency. The IRC paths were traced in order to check the energy profiles connecting each TS to the two associated minima of the proposed mechanism using the second order González–Schlegel integration methods. Values of free energies in chloro-form were calculated with standard statistical thermodynamics under reaction conditions. Solvent effects of chloro-form on the thermodynamic calculations were considered by using a self-consistent reaction field (SCRF) based on the polarizable continuum model (PCM) of the Tomasi's group. All computations were carried out with the Gaussian 09 suite of programs (Frisch *et al.*, 2009).

The theoretical cartesian coordinates for the *thione* and *thiol* dimers, as well as for the Transition State for double proton transfer are included as Supporting Information Tables ST1, ST2 and ST3.

3. Results and discussion

3.1. NMR analysis

Tautomeric equilibria are most noticeable in solution, and ^{1}H-NMR is a very adequate tool for its detection. Fig. 1(a) shows the ^{1}H-NMR spectrum in $CDCl_3$ (at RT), where it is possible to see the signals of the protons attached to the nitrogen atoms of the heterocyclic ring, indicating that *thione* structure is present (hydrogens 1c and 3c). In addition, at high field, it is possible to detect a maximum (*c.a.* 1.7 ppm, H—S in the figure), which is characteristic of a proton attached to the sulfur atom, indicating likewise the presence of the *thiol* structure.

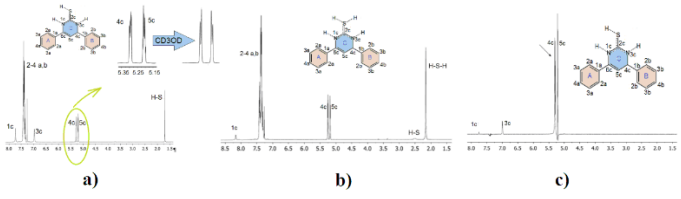

Figure 1. a) 1H-NMR spectrum of I in $CDCl_3$. b) After addition of CD_3OD. c) TOCSY experiment, irradiation in 5.29 ppm.

So there are two protons to locate, and the tautomeric equilibrium offers three positions for them. Then, in case the tautomeric equilibria were equimolar for both structures, the integration of the proton signals would be 0.67 (2/3) for each one; however, an integration of 0.7 is observed for each proton of the thione structure and 0.6 for the thiol structure; although it is always possible to argue whether this difference falls within the margin of experimental error, it would thus be seen that the thione form is slightly favored at this equilibrium in solution.

Since aromatic protons are well identified (the overlapping picks around 7.32-7.44 ppm), the focus of the search was placed on the central heterocycle ones, and in this regard several experiments were carried out in order to correlate exactly each maximum with the corresponding proton.

To identify protons 4c and 5c beyond any doubt a TOCSY experiment with energy corresponding to 5.29 ppm was carried out. Fig 1(c) shows the corresponding spectrum. The possible combinations relating the peaks give rise to the identification shown in the figure, viz.: 4c coupled to protons 5c and 3c, and only weakly with proton 1c, which is further away. In this way, the identity of those protons linked to nitrogen atoms was resolved.

The neighboring protons 4c and 5c (attached to the vinyl and allyl carbon atoms respectively) are coupled together; however, they are also coupled with other protons, such as those bonded to the nitrogen atoms, 1c and 3c. This causes that the maxima corresponding to these protons are not simple doublets, but have a higher multiplicity (see insert of Fig 1(a) and full spectrum in Fig 1(b)); however, when deuterated methanol is added to the system, this coupling disappears; then the signals of protons 4c and 5c transform into doublets. The interpretation is that the protons belonging to the nitrogen atoms leave the molecule when immersed in a more polar environment, as the one generated by the addition of methanol and which allows protons to express their acidic behavior.

Theoretical calculations (DFT level) show that the most acidic proton (the first to leave the molecule), is 3c. 1H-NMR analysis suggest that this proton migrates to the S nearby and generates a weak S—H signal at 2.50 ppm (see Fig. 1b); furthermore, the signal from proton 1c is shifted to a smaller field (from 7.72 to 8.16 ppm, see Fig. 1c).

On the other hand, due to being in a more polarized environment, both NH protons would migrate towards the sulfur atom; as a consequence, proton signals 1c and 3c would tend to disappear (in the spectrum, the integration of both protons is much less than 1), resulting in a signal at 2.16 ppm, which integrates by two protons, suggesting that the H—S—H structure with two protons attached to the sulfur atom represents the major fraction, the one with a single proton being only marginal.

In brief, NMR experiments demonstrate that both tautomeric structures are present in solution.

3.2. FTIR analysis

The detection of the tautomeric equilibrium is much more difficult in the solid state, and an extremely useful tool for this effect is FTIR,. Fig.2. shows a superposition of the experimental spectrum of I (at RT) and the theoretical spectra of the two tautomeric forms, calculated through theoretical methods at the DFT level. Analysis of the figure discloses the presence of both tautomeric forms: on one side, the thiol one, through two bands assignable to the S—H bond and the C=N double bond. On the other side, the expected thione form, through a typical S=C stretching band. The information is summarized in Table 1, which presents the most important bands revealing the presence of the characteristic functional groups and demonstrating (at least qualitatively) that both tautomeric structures are also present in the solid state at room temperature. However, a quantitative assessment is much more difficult in this case than in solution.

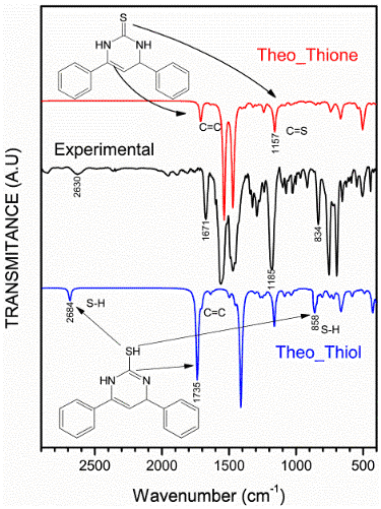

Figure 2. FTIR of I.

Table 1. Some important IR bands, which reveal the presence of the functional groups characteristic of both tautomeric forms

Thiol	experimental	Theoretical
S—H bond	2639 cm^{-1} (stretching)	2717 cm^{-1}
	832 cm^{-1} (bending)	895 cm^{-1}
C=N	1673 cm^{-1} (stretching)	1613 cm^{-1}
Thione	**experimental**	**Theoretical**
S=C	1187 cm^{-1} (stretching)	1157 cm^{-1}

3.3. X-Ray analysis

Even in the knowledge that we were pushing the possibilities of the method to its limits we undertook the SCXRD study of I, trying to gain some further insight into the tautomeric problem in the solid state. The compound crystallizes in the triclinic space group P-1, with 6 molecules in the unit cell and 3 independent moieties in the asymmetric unit (z=6, z'=3). Fig 3 shows the (similar) labelling scheme used for them, just differentiated in the trailing letter (A, B, C), while Table 2 affords some crystallographic details.

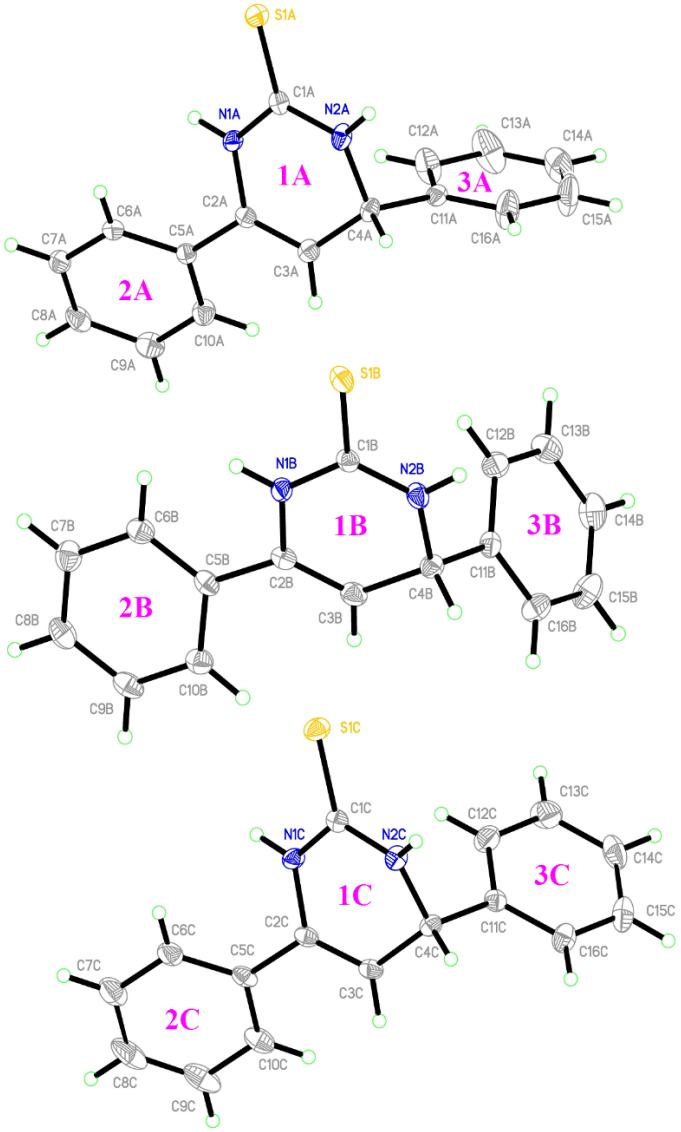

Figure 3. Molecular diagram representative of all three moieties, showing the (similar) labelling scheme used for them, just differentiated in the trailing letter (A, B, C).

Table2. Experimental details

Crystal data	
Chemical formula	$C_{16}H_{14}N_2S$
M_r	266.35
Crystal system, space group	Triclinic, $P\bar{1}$
Temperature (K)	170
a, *b*, *c* (Å)	11.3028 (3), 11.8740 (4), 17.3081 (5)
α, β, γ (°)	87.691 (1), 72.942 (1), 65.891 (1)
V (Å^3)	2018.57 (11)
Z	6
Radiation type	Mo *K*α
μ (mm^{-1})	0.23
Crystal size (mm)	0.28 × 0.16 × 0.14

Data collection	
Diffractometer	Bruker *SMART* AXS CCD diffractometer
Absorption correction	Multi-scan '*SADABS* (Bruker, 2002)'
T_{min}, T_{max}	0.50, 0.85
No. of measured, independent and observed [$I > 2\sigma(I)$] reflections	59437, 11260, 9358
R_{int}	0.032
$(\sin\theta/\lambda)_{max}$ ($Å^{-1}$)	0.709

Refinement	
$R[F^2 > 2\sigma(F^2)]$, $wR(F^2)$, *S*	0.027, 0.062, 1.04
No. of reflections	11260
No. of parameters	532
No. of restraints	6
H-atom treatment	H atoms treated by a mixture of independent and constrained refinement
$\Delta\rho_{max}$, $\Delta\rho_{min}$ (e $Å^{-3}$)	0.25, -0.18

Computer programs: *SMART-NT* (Bruker, 2001), *SAINT-NT* (Bruker, 2002), *SAINT-NT* (Bruker, 2002), *SHELXS97* (Sheldrick, 2008), *SHELXL2014*/6 (Sheldrick, 2015), *XP* in *SHELXTL* (Sheldrick, 2008), *SHELXL2014*/6, *PLATON* (Spek, 2009).

An early result of the structural resolution was the finding that the central skeleton of the molecule consists of a tetra-hydro-pyrimidine group, thus confirming previous NMR results which clarified the initial S *vs.* N synthetic uncertainty. To this skeleton there are two further phenyl rings attached at sites 4 and 6 and a sulfur atom bound at site 2. Table 3 presents quantitative data assessing the planarity of these groups. As expected from their aromatic character, phenyl rings 2 and 3 present very small deviations from the mean plane (maximum departures: 0.016 (2)Å in ring 2A and 0.013 (2)Å in 3C). A more interesting situation arises with Ring 1, which pseudo-planarity is not due to aromaticity but to the substitution scheme, instead. In spite of this, departures for A and C are small (max: 0.090 (2)Å and 0.155 (2), respectively), but even so are large when compared with ring B, which presents deviations even smaller than those for its aromatic neighbours 2 and 3.

Table 3. Individual deviations (Å) from the mean plane in Rings 1,2 and 3.

Ring 1	N1	N2	C1	C2	C3	C4
A	-0.068 (1)	0.058 (1)	0.023 (1)	0.021 (1)	0.056 (2)	-0.090 (1)
B	-0.008 (2)	-0.001 (2)	0.009 (2)	-0.001 (2)	0.008 (2)	-0.006 (2)
C	0.100 (1)	-0.148 (1)	0.016 (2)	-0.068 (2)	-0.055 (2)	0.155 (2)

Ring 2	C5	C6	C7	C8	C9	C10
A	-0.012 (2)	0.013 (2)	0.001 (2)	-0.015 (2)	0.016 (2)	-0.003 (2)
B	0.000 (2)	-0.012 (2)	0.012 (2)	-0.001 (2)	-0.011 (2)	0.011 (2)
C	0.009 (2)	-0.009 (2)	0.000 (2)	0.009 (2)	-0.008 (2)	-0.001 (2)

Ring 3	C11	C12	C13	C14	C15	C16
A	0.001 (2)	0.000 (2)	0.000 (2)	-0.001 (2)	0.003 (2)	-0.003 (2)
B	0.003 (2)	-0.002 (2)	-0.001 (2)	0.003 (2)	-0.002 (2)	-0.001 (2)
C	0.004 (2)	-0.009 (2)	0.003 (2)	0.008 (2)	-0.013 (2)	0.007 (2)

The independent molecules are metrically similar, with no significant differences in bond distances (Supporting Information Table ST4) or angles (Supporting Information Table ST5). The main discrepancies appear in the torsion angles, a fact to be expected from having two phenyl groups attached with unimpeded rotation. The analogies and differences are better assessed in the superposition diagram shown in Fig 4. Only the atoms in the central core were used for fitting, which superimpose with just small departures; the eventual details differentiating the rest are apparent. Rings type 2 (C5—C10) are rotated by different amounts out of the plane defined by the central ring, around the C2—C5 bond (see Table 4, first column). Inspection of Fig.4 suggests this is the only type of deformation present, the C2—C5 bond keeping nearly in the N1—C2—C3 plane (dev.: 0.8, 1.7 and 2.2°, for A, B, C, respectively) thus confirming the sp2 character of atom C2.

Table 4. Dihedral angles subtended by the central tetrahydropyrimidine group (1X) to the lateral phenyl rings (2X,3X), X = A, B, C.

1A, 2A	22.83 (8)	1A, 3A	86.11 (9)
1B, 2B	17.73 (9)	1B, 3B	74.96 (9)
1C, 2C	23.23 (8)	1C, 3C	79.67 (8)

Atom C4, instead, presents an sp3 hybridization, with more degrees of freedom which allows group 3 to differ not only in its unimpeded rotation, but in bending as well, a fact which appears clear from inspection of Fig 4.

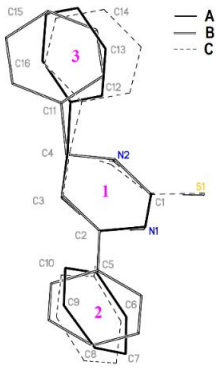

Figure 4. Superposition diagram of the thee moieties. Only the atoms in the central core were used for fitting.

Regarding the crystal structure organization, it is directed by the six N—H···S hydrogen-bonds, presented in Table 5, where, for convenience, they have been identified by an individual code (#1 to #6, first column). Through this H-bonding scheme each A, B or C molecule is connected to two different ones through two different N—H···S bonds forming $R^2_2(8)$ rings and thus defining A≈B, B≈C and C≈A dimers (where ≈ represents the $R^2_2(8)$ loop), concatenated along chains which run along [1^{-}10]. Fig.5a presents a highly simplified scheme of these chains (phenyl rings removed), which allows to follow its spatial evolution. Figure 6, in turn, is intended to show the complexity of the resulting full array, shown in projection along the chains, and where one of these columns has been highlighted, for an easy identification.

From the figure it is clear the tight columnar inbreeding having place, which leads to a number of weaker inter-chain interactions mainly of the C—H···π type (#7 to #9 in Table 5, not shown in the Figure) and which results is the final 3D structure.

Table 5. Hydrogen-bond geometry (Å, °)

Code	*D*—H···*A*	*D*—H	H···*A*	*D*···*A*	*D*—H···*A*
#1	N1A—H1A···S1C^{i}	0.852 (9)	2.896 (9)	3.7442 (14)	173.4 (16)
#2	N2A—H2A···S1B^{ii}	0.858 (9)	2.450 (11)	3.2680 (14)	159.8 (17)
#3	N1B—H1B···S1C^{iii}	0.864 (9)	2.736 (9)	3.5947 (14)	173.3 (16)
#4	N2B—H2B···S1A^{ii}	0.858 (9)	2.628 (10)	3.4568 (15)	162.7 (16)
#5	N1C—H1C···S1B^{iii}	0.851 (9)	2.530 (10)	3.3745 (14)	171.8 (17)
#6	N2C—H2C···S1A^{iv}	0.844 (9)	2.534 (10)	3.3605 (14)	166.6 (16)
#7	C4A—H4A···Cg3C	0.93	2.71	3.648 (2)	159
#8	C4C—H4C···Cg2C^{v}	0.93	2.55	3.435 (2)	150
#9	C8B—H8B···Cg2A	0.93	2.76	3.527 (2)	140

Symmetry codes: (i) x, y-1, z; (ii) -x, -y+1, -z+1; (iii) -x+1, -y+1, -z+1; (iv) x, y+1, z; (v) -x+1, -y+1, -z.

Cg2A: C5A, C6A, C7A, C8A, C9A, C10A; Cg2C: C5C, C6C, C7C, C8C, C9C, C10C; Cg3C: C11C, C12C, C13C, C14C, C15C, C16C.

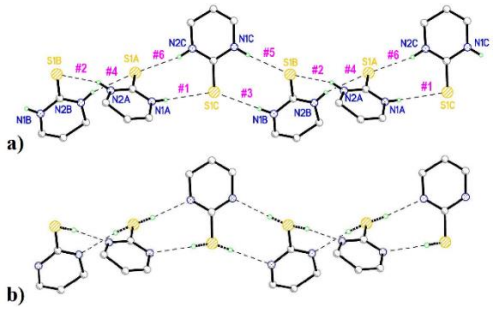

Figure 5. a) A highly simplified scheme of the chains (phenyl rings removed), with H-bonds bonds in broken lines. b) a plausibility argument of the way the tautomeric equilibrium could be achieved through hydrogen atoms "captured" by their neighbouring sulfurs, in a disordered, minoritarian, fashion.

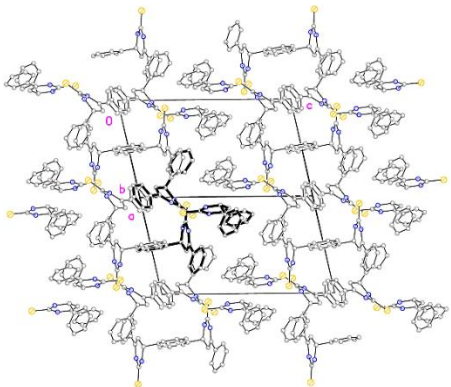

Figure 6. A packing view of (I) drawn in projection along the chain axis. One of the columns has been highlighted, for an easy identification.

As already commented above, we had already collected evidence about isomeric coexistence of S—H ⇌ N—H states, both in solution (NMR) as in the solid state (FTIR). Even if a quantitative evaluation of the existing fractions could be made in the first case, via integration of the proton signals, this evaluation in the latter case is much more elusive, the detection being basically qualitative in nature.

In order to find out any possible vestige of this effect in the crystal structure, difference maps were calculated around the sulfur atoms and were carefully analyzed in search of any eventual disordered H atom. The efforts ended up being fruitless, with the final conclusion that the effect, even if present in the solid state (at room temperature) as assessed by FTIR, in the low temperature conditions in which the SCXRD experiments were performed appears beyond detection. In any case, this is not a surprising result: a search in the CSD of similar S(C_4N_2) backbones as in I (Scheme 2a), leaving unrestricted the type of bonds but subjected to the restriction that only H's would eventually bind N (Scheme 2b) or S (Scheme 2c) threw ca 300 hits, of which only two cases were deemed to exhibit a C—S—H group, but in none of which the H's had been experimentally found.

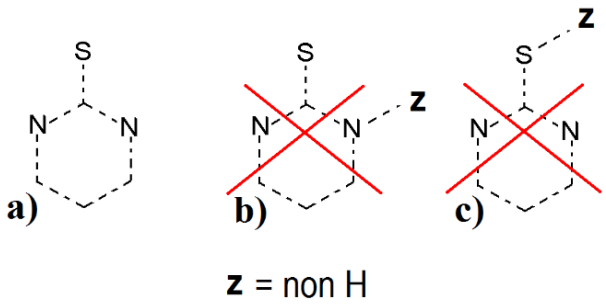

Scheme 2

However, the analysis of the crystal structure allows for some plausible speculations about the way in which the coexistence in the solid (confirmed by FTIR) could take place. To begin with, this could only take place through a depletion of the H population in the NH groups in the heterocycle. We thus indulged in a (perhaps foolhardy..!) refinement of the occupation factors of the N—H's, somehow speculating with the extremely good quality of the data set, and just in order to see what happened. To our surprise, all six H's returned sensible occupation values, slightly below unity and with a reasonably small span (range: 0.93-0.97).

In parallel, the analysis of Fig 5a suggests that each sulfur atom, in its role of double "receiver" of N—H···S bonds, could in fact be a "physical acceptor" of the fraction of H's lost by the N's (and which would then have migrated to the S neighbourhood along the N···S line). As a consequence, the S atom would become an H-bond donor, and the corresponding interaction, in turn, a N···H—S one. Fig.5b gives a plausibility idea of the way this could be achieved, through each S atom "capturing" in a disordered way (only one of the two S—H bonds shown in broken lines could exist at a time) and in an extremely low fraction (in fact, the one given by the *thiol/thione* equilibrium ratio) the H atom of its former donors. Even if the preceding argument was highly speculative, it served as the starting point for the theoretical calculation below, which showed its plausibility at the same time which it provided quantitative details clarifying the tautomeric equilibrium in solution.

Crystallographic data has been deposited at the CCDC under code CCDC1823685. These data can be obtained free of charge via the CCDC retrieval website http://www.ccdc.cam.ac.uk/conts/retrieving.html.

3.4. Theoretical Study

For the theoretical calculations we have used (as suggested by the structural data already discussed) a dimeric model, in which a double proton transfer occurs. It is to be noted that similar models have already been used in the literature, viz., in Özdemir, 2013.

The computational study carried out at the B3LYP/6-311G(d,p) level of theory showed good agreement between the experimentally obtained crystal structure and the calculated ones, with the expected differences derived from the different media: the calculations being based on isolated molecules in the gas and solution phase, while the experimental results arise from the solid state. The schematic energy profile of the double proton transfer process (Fig. 7) shows an energy difference ΔG_1 = 33.8 kcal mol^{-1} between both tautomeric forms. This value agrees with those found in similar systems (e.g. Özdemir, 2013).

For this dimeric model, the involved S—H and H—N distances in the S···H···N arrangement for the proposed transition state are 1.44 Å and 1.62 Å respectively (Fig.7); which seem much energetically more convenient than an intra-molecular transfer of a single proton.

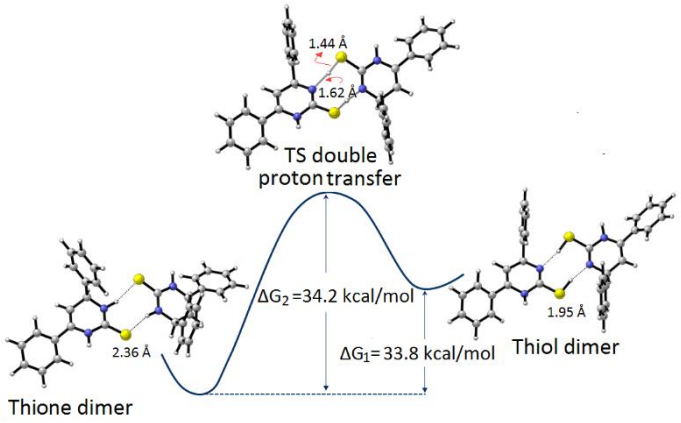

Figure 7. Energy profile of the single proton transfer process, showing the thione tautomer to be more stable than the thiol one.

Document origin: publCIF [Westrip, S. P. (2010). J. Apply. Cryst., 43, 920-925]. In addition, the free energy of the TS was found to be ΔG_2 = 34.2 kcal mol^{-1}; the resulting energy barrier $\Delta G_2 - \Delta G_1$ is thus small enough as to be easily overcome at room temperature, allowing the *thiol* form to transform into the most stable thione one. These results, obtained from a model in solution, are absolutely compatible with what found by SCXRD in the solid, where very short S···H distances were found (see entries #1 to #6 in Table 5 and Fig 5). The small energy barrier could explain the different results obtained by FTIR, performed at room temperature, with enough energy in the system as to allow for an incipient presence of the *thiol* form, in contrast to SCXRD, performed at 170K, with a different scenario, mainly frozen in the lower, *thione* side of the barrier.

CONCLUSION

Compound I, 4,6-di-phenyl-3,4-di-hydro-pyrimidine-2(1H)-thione, has been synthesized and its crystal and molecular structure determined. Room temperature NMR and FTIR experiments allowed to assess that this molecular system exhibits a *thione-thiol* equilibrium both in solution as in the solid. The connectivity of the molecules in this latter state as determined through SCXRD at 170K served as the basis for a computational model which provided quantitative estimations of the relative energy of each species as well as the energetic barrier which separates them. From these values it is concluded that the *thione* species is the most stable one.

The results obtained suggest further complementary courses of action to pursue, at present beyond our experimental capabilities (*e.g.*, FTIR at liquid N_2 temperature, or even a single crystal neutron scattering analysis at variable temperature). For the time being, we are forced to leave this as a wishfull perspective.

It is thus concluded that X-ray diffraction, although it is the main test of a certain structural arrangement, in specific problems it must be supported by other techniques, such as NMR and/or FTIR, which finally tip the balance towards one or another molecular structure.

ACKNOWLEDGEMENTS

This research has been performed as part of the French-Chilean International Research Project "Cooperation in Inorganic Chemistry" (IRP CoopIC). Dirección de Investigación y Desarrollo de Universidad de La Serena, DIDULS (proyecto N° PAAI214).

REFERENCES

1. Frisch, M. J., *et al.* (2009). *GAUSSIAN09*. Gaussian Inc., Wallingford, CT, USA. http://www.gaussian.com.
2. Groom, C. R., Bruno, I. J., Lightfoot, M. P. & Ward, S. C. (2016). *Acta Cryst.* B**72**, 171–179.
3. Gupta, P. & Gupta, J. (2015). *Chem Sci J.* **6**, 2-12.
4. Kachroo, M., Panda, R. & Yadav, Y. (2014). *Der Pharma Chemica*, **6**, 352-359.
5. Kong, K. H., Chen, Y., Ma, X., Chui, W. K. & Lam, Y. (2004). J. Comb. Chem. 6, 928-933.
6. Özdemir, N. & Türkpençe, D. (2013). Computational and Theoretical Chemistry 1025, 35–45.
7. Bruker (2002). *SAINT-NT* V6.22a (Including *SADABS*). Data Reduction Software. Siemens Analytical X-ray Instruments Inc., Madison, Wisconsin, USA.
8. Bruker (2001). *SMART-NT* V5.624. Data Collection Software. Siemens Analytical X-ray Instruments Inc., Madison, Wisconsin, USA.
9. Sheldrick, G. M. (2008). *Acta Cryst.* A**64**, 112–122.
10. Sheldrick, G. M. (2015). Acta Cryst., C**71**, 8–15.
11. Spek, A. L. (2009). *Acta Cryst.* D**65**, 148–155.
12. Stoyanov, S., Petkov, I., Antonov, L., Stoyanova, T., Karagiannidis, P. & Aslanidis, P. (1990). *Canadian Journal of Chemistry*, **68**, 1482-1489. 7.
13. Trivedi, M. K., Branton, A., Trivedi, D., Shettigar, H., Bairwa, K. & Jana, S. (2015). Nat Prod Chem Res, 3:186.
14. Zeng, R.-S., Zou, J.-P., Zhi, S.-J., Chen, J. & Shen, Q. (2003). *Organic Letters*, **5**, 1657-1659.
15. Zhang, L., Peng, X.-M., Damu, G. L. V., Geng, R.-X. & Zhou, C.-H. (2014). *Medicinal Research Reviews*, **34**, 340-437.